International Journal of Mass Spectrometry 307 (2011) 214–224

Contents lists available at ScienceDirect

International Journal of Mass Spectrometry

journal homepage: www.elsevier.com/locate/ijms

Mercury isotope fractionation during abiotic transmethylation reactions

D. Malinovsky*, F. Vanhaecke

Department of Analytical Chemistry, Ghent University, Krijgslaan 281-S12, B-9000 Ghent, Belgium

ARTICLE INFO

Article history:
Received 12 November 2010
Received in revised form 18 January 2011
Accepted 18 January 2011
Available online 2 February 2011

Keywords:
Mass-dependent and mass-independent isotope effects
MC-ICPMS
Photochemical methylation

ABSTRACT

Experiments modeling abiotic methylation of mercury were performed by using methylcobalamin, methyltin, acetic acid and dimethylsulfoxide as the methyl donor compounds. Mercury isotope ratios were measured by using multicollector ICP-MS for both methylmercury and parent inorganic Hg(II). Abiotic methylation of mercury in the dark was accompanied by mass-dependent Hg isotope fractionation with isotope fractionation factors, $\alpha_{product/substrate}$, ranging from 0.9985 to 0.9995 in terms of $\delta^{202/198}$Hg values and with undetectable Hg isotope anomalies. The radical substitution reactions, releasing a methyl radical in solution in the dark, facilitated formation of methylmercury and increased the magnitude of the concomitant mass-dependent Hg isotope effect but were not capable of producing any measurable mass-independent anomaly in the isotopic composition of mercury. In contrast to methylation in the dark, photochemical methylation of mercury was accompanied by both mass-dependent and mass-independent Hg isotope fractionation. The latter resulted in selective enrichment of ^{199}Hg and ^{201}Hg isotopes in methylmercury and was attributed to the magnetic isotope effect. These data highlight the fact that the light-assisted methylation of mercury produces a unique mass-independent Hg isotope signature that can be used in tracing the origin of this highly toxic compound.

1. Introduction

Mercury occurs naturally in the environment and exists in different chemical forms including elemental mercury, inorganic and organic mercury species. Due to its high toxicity, mercury is considered internationally as a priority pollutant. Among the most toxic forms of the element is methylmercury. It has been shown by numerous authors that methylation of mercury occurs in natural waters by means of both biotic and abiotic processes [1,2]. Microbially assisted processes are major routes for formation of methylmercury in natural waters [2]. However, uncertainty still remains to what extent the purely chemical process contributes to the methylation of mercury. As a complex interplay of biotic and abiotic processes occurs in the environment, it is difficult to differentiate between various contributions from abiotic and biological processes in the formation of methylmercury. However, this knowledge is crucial in understanding of biogeochemical cycling of Hg.

A promising tool in understanding pathways of transformations between different chemical forms of Hg in the environment is the use of its isotope data. Recent reports from many research groups have demonstrated that major physico-chemical transformations of mercury in the environment are concomitant with variations in the isotopic composition of the element ([3–5] and references therein). Apart from the classical, mass-dependent isotope fractionation, anomalous or mass-independent fractionation (MIF) of Hg isotopes has been reported for biological samples, sediments, soils and coal [4–7]. MIF of Hg isotopes have been experimentally observed during photochemical reduction of Hg(II) to the elemental state in the presence of dissolved organic matter [8–10], transformation of metallic Hg^0 into gaseous Hg^0 [11] and photodissociation of methylmercury [12]. A case of in vivo MIF of Hg isotopes in fish has also been reported [13]. Experimental studies have demonstrated that methylation of inorganic mercury by microorganisms [14], biotic Hg(II) reduction and demethylation of methylmercury have shown mass-dependent pattern of Hg isotope fractionation with the complete absence or unresolvable MIF [15,16].

The isotope effects of Hg during purely chemical methylation have not yet been studied. Thus, the research described here was aimed at evaluating the extent of Hg isotope fractionation during transmethylation reactions of inorganic Hg(II) with selected methyl group donors which can be present in natural aquatic environments. These compounds include methyltin, methylcobalamin, acetic acid and dimethylsulfoxide (DMSO). A methyl group can be transferred from a donor compound to an acceptor, including Hg, as a cation (CH_3^+), anion (CH_3^-) or radical ($CH_3^\bullet$) [17,18]. These different pathways of methylmercury production have been experimentally modeled in order to study the concomitant Hg isotope fractionation. A special emphasis has been given to modeling Hg isotope fractionation during transfer of a methyl group to mercury as a radical. This is because the interactions between radicals, including recombination of radical pairs, form the basis for the

* Corresponding author. Tel.: +32 9 2644824; fax: +32 9 2644960.
E-mail address: dmitry.malinovskiy@ugent.be (D. Malinovsky).

1387-3806/$ – see front matter © 2011 Elsevier B.V. All rights reserved.
doi:10.1016/j.ijms.2011.01.020

occurrence of the magnetic isotope effect. The latter is considered to be one of the primary mechanisms responsible for the mass-independence of Hg isotope fractionation.

Although the concentration of Hg used in the experiments was higher that that in natural waters, this study under controlled laboratory conditions allows us to determine the extent of Hg isotope fractionation and make inferences on its mechanisms.

2. Experimental

2.1. Instrumentation

Prior to Hg isotope ratio measurements, the concentration of Hg was determined using single-collector sector field instrument (Element 2, Thermo Scientific, Germany). The instrumental uncertainty associated with Hg concentration measurements ranged from 0.3% to 2% at 70% confidence (1σ) level. After concentration of Hg had been determined, the samples were diluted with 0.3 M HNO_3 containing 0.1% L-cysteine to match Hg concentrations with isotope standards to within 25% and spiked with Tl to correct for instrumental mass discrimination at ~1/8 of the Hg concentration to match the intensity of $^{202}Hg^+$ and $^{205}Tl^+$ signals. Hg and Tl isotope ratios were measured by multicollector ICP-MS (MC-ICPMS; Thermo Scientific, Germany), largely following the approach described in detail previously [12,19]. Prior to each measurement session, the instrument was carefully tuned to maximize the intensity of Hg signal by adjusting the torch position, gas flow rates and lens voltages. Samples and standards were introduced into plasma via a stable introduction system consisting of a peristaltic pump, a micro-concentric PFA nebulizer, and a tandem quartz spray chamber arrangement (cyclone + Scott double pass). ^{198}Hg, ^{199}Hg, ^{200}Hg, ^{201}Hg, ^{202}Hg, ^{203}Tl, and ^{205}Tl isotopes were collected by Faraday cups at low 3, low 2, low 1, central, high 1, high 2, and high 3 positions, respectively. Typical sample measurement consisted of 6 blocks, each block comprising 7 cycles of ~4.2 s duration. Analyses were carried out in a "bracketing" sequence of isotopic standard, "unknown" sample, isotopic standard, and so on. To avoid memory effects from previous solutions, it was always verified in the on-line "scan window" that ^{202}Hg signal from the previous sample dropped to the blank level of ~0.005 V before starting the measuring sequence for the next sample. All samples were run in duplicate. The instrumental precision for Hg isotope ratio measurements was less than 0.10‰, 0.09‰, 0.10‰ and 0.12‰ for $^{199}Hg/^{198}Hg$, $^{200}Hg/^{198}Hg$, $^{201}Hg/^{198}Hg$ and $^{202}Hg/^{198}Hg$ ratios, respectively, at 70% confidence (1σ) level. Standard Reference Material NIST-3133 (Hg standard solution, Lot No. 061204) was used as the isotope standard in this work.

2.2. Isotope ratio data reduction and presentation

The on-line data processing included calculation of the ion beam intensity ratios and filtering of outliers by a 2σ test. Further treatment of the isotope ratio data was performed off-line. Instrumental mass discrimination was corrected for by using an exponential model as described in detail elsewhere [20]. Results for the isotopic analyses are expressed in the δ-notation, as defined by the relationship

$$\delta^{X/198}\mathrm{Hg} = \left[\frac{(^{X}\mathrm{Hg}/^{198}\mathrm{Hg})_{\mathrm{sample}}}{(^{X}\mathrm{Hg}/^{198}\mathrm{Hg})_{\mathrm{standard}}} - 1\right] \times 1000\ ‰ \quad (1)$$

where ^{X}Hg is ^{199}Hg, ^{200}Hg, ^{201}Hg and ^{202}Hg isotopes, respectively, in the measured ratios for sample and standard, corrected for instrumental mass discrimination using Tl ($^{205}Tl/^{203}Tl = 2.3871$). Apart from the conventional δ-notation, capital delta notation was also used to describe mass-independent fractionation of Hg isotopes as defined by Blum and Bergquist [21]

$$\Delta^{199}\mathrm{Hg} = \delta^{199}\mathrm{Hg} - 0.2520 \times \delta^{202}\mathrm{Hg} \quad (2a)$$

$$\Delta^{201}\mathrm{Hg} = \delta^{201}\mathrm{Hg} - 0.7520 \times \delta^{202}\mathrm{Hg} \quad (2b)$$

where coefficients of 0.252 and 0.752 represent values of fractionation exponent, β, expected for kinetic mass-dependent fractionation of isotopes involved in the equations above. By using masses of the isotopes (m), these values are calculated as follows [22]:

$$\beta_1 = \frac{\ln[m(^{198}\mathrm{Hg})/m(^{199}\mathrm{Hg})]}{\ln[m(^{198}\mathrm{Hg})/m(^{202}\mathrm{Hg})]} = 0.2520 \quad (3a)$$

$$\beta_2 = \frac{\ln[m(^{198}\mathrm{Hg})/m(^{201}\mathrm{Hg})]}{\ln[m(^{198}\mathrm{Hg})/m(^{202}\mathrm{Hg})]} = 0.7520 \quad (3b)$$

Measured differences in the isotopic composition of methylmercury and inorganic mercury during methylation can be related to isotope fractionation factor, $\alpha_{\mathrm{product/substrate}}$, in terms of $^{202}Hg/^{198}Hg$ isotope ratio as follows:

$$\alpha = \left(\frac{1000 + \delta^{202/198}\mathrm{Hg}_{\mathrm{product}}}{1000 + \delta^{202/198}\mathrm{Hg}_{\mathrm{substrate}}}\right) \quad (4)$$

Following terminology from an experimental study by Skulan et al. [23], we define the instantaneous isotope fractionation in the experiments as $\alpha^{\mathrm{I}}_{\mathrm{product/substrate}}$, where $\delta^{202/198}\mathrm{Hg}_{\mathrm{product}}$ and $\delta^{202/198}\mathrm{Hg}_{\mathrm{substrate}}$ are isotopic delta values for methylmercury and parent inorganic mercury at the time of sampling, respectively.

Where possible, we also inferred kinetic isotope fractionation factor, $\alpha^{\mathrm{K}}_{\mathrm{product/substrate}}$, during unidirectional reaction using the classical Rayleigh distillation equation which in per mil notation takes form [24,25]

$$(\alpha^{\mathrm{K}} - 1)\ln f = \ln\frac{10^{-3}\delta_{\mathrm{s}} + 1}{10^{-3}\delta_{\mathrm{s},0} + 1} \quad (5)$$

where α^{K} is the kinetic isotopic fractionation factor which is considered as a constant during the course of reaction; f is the fraction of inorganic mercury remaining in solution; $\delta_{\mathrm{s},0}$ and δ_{s} are isotopic delta values for inorganic mercury at the beginning of the process and at a time of sampling, respectively.

2.3. Materials and reagents

High-purity deionized water was obtained from Milli-Q water purification system (Millipore, USA). Hydrochloric and nitric acids were purified in-house by sub-boiling distillation of reagent grade feedstock using a quartz (for HCl) or PFA (for HNO_3) still. A 0.18 M BrCl solution was prepared in a fume hood by dissolving 0.27 g of KBr (Merck, Darmstadt, Germany) in 25 ml of 10 M HCl and then slowly adding 0.38 g of $KBrO_3$ while stirring. Chelating ion-exchange resin Chelex® 100, 200–400 mesh (Bio-Rad, analytical grade), AG-MP-1 M anion-exchange resin, 100–200 mesh size, methylcobalamin, monomethyltin and other chemicals were obtained from Sigma Aldrich. All calibration and internal standard solutions used were prepared by diluting single-element standard solutions (Merck, Germany).

2.4. Experimental design

In order to model different reaction pathways of methylmercury formation, three types of experiments have been performed. The first type includes methylation reaction between inorganic Hg(II) and the methyl group donors in the dark. Inorganic mercury (dilute NIST reference material SRM-3133, Hg standard solution), ranging in concentration from 0.5 μM to 5 μM, was added into 20-ml glass

vial with caps, following addition of ~100 time higher quantity of one of the methyl group donors used, i.e., methyltin, methylcobalamin, acetic acid or dimethylsulfoxide (DMSO). pH values were adjusted by using dropwise addition of dilute NaOH and HCl. The reaction vials have been wrapped in aluminum foil and kept with stirring during time intervals ranging from 24 h to 96 h.

In the second type of the experiments, the reaction of inorganic Hg(II) with the methyl group donor compounds has been studied in the dark with the presence of hydroxyl radicals generated by the Fenton type reaction. The latter is based on efficient conversion of hydrogen peroxide to hydroxyl radical according to the following reaction scheme [26]

$$H_2O_2 + Fe^{3+} \rightarrow HO_2^{\bullet} + Fe^{2+} + H^+ \quad (6a)$$

$$H_2O_2 + Fe^{2+} \rightarrow OH^{\bullet} + OH^- + Fe^{3+} \quad (6b)$$

The highly reactive hydroxyl radical ($OH^{\bullet}$) interacts indiscriminately with organic compounds, resulting in homolytic cleavage of both carbon–carbon and organometallic bonds and producing, among other intermediate species, a methyl radical ($CH_3^{\bullet}$) [27]. Production of $CH_3^{\bullet}$ due to reaction with hydroxyl radicals has been documented for methylcobalamin, acetic acid, and DMSO [28–30]. Provided that the concentration of hydroxyl radicals is not too high, the radical substitution reactions, generating $CH_3^{\bullet}$, can facilitate methylation of mercury. These experiments followed the same protocol as in the first type, except that H_2O_2 at a concentration ranging from 1 to 5 mM and $FeCl_3$ at a concentration of 0.5 mM were added to the solutions in order to initiate the Fenton type reaction.

The third type of the experiments was designed to model photochemical methylation of mercury. It was demonstrated previously that methylmercury can be produced by reaction of inorganic Hg(II) with dissolved organic matter, including acetic and propionic acids, under irradiation with sunlight or ultraviolet light [17,31]. The experiments used the same amounts of the reagents as those in the dark. The sample vials were positioned directly under a 325 nm ultraviolet (UV) lamp (30 W, Philips TUV, Holland). The duration of UV irradiation varied between 15 and 45 min.

2.5. Ion-exchange chromatography

At the end of each experiment, methylmercury was separated from parent inorganic mercury by ion-exchange chromatography, following the approach described in detail by Malinovsky et al. [12], with minor modifications. The ion-exchange columns were prepared from 5 ml pipette tips, fitted with plugs of cotton wool at the outlets and filled with ~1 ml of Chelex® 100, 200–400 mesh size ion-exchange resin. Prior to use the ion-exchange column was cleaned with 1 M HNO_3 and conditioned with a solution of 0.5 M HCl/70% MeOH. Typically, 28 ml of MeOH and 2 ml of 10 M HCl were added into 50 ml polyethylene vials followed an addition of 10 ml of the sample solution. This methanolic solution was then transferred onto the preconditioned ion-exchange column. The ion-exchange separation of methylmercury from inorganic Hg(II) makes use the fact that in dilute hydrochloric medium methylmercury exists as neutral CH_3HgCl complexes and passes through the column, whereas inorganic Hg(II) in the forms of charged $HgCl_3^-$ and $HgCl_4^-$ complexes retained on the resin. As advocated previously [12], addition of methanol is important in minimizing sorption of methylmercury on the ion-exchange resin. The inorganic Hg(II) was eluted from the column by using 8 ml of 0.1 M HNO_3 solution containing 0.15% L-cysteine and 0.001 M BrCl.

The separated fraction of methylmercury was quantitatively converted into inorganic Hg by adding freshly prepared BrCl at 3% concentration level. The solution was then kept on a hot plate at 60–70 °C in order to get rid of methanol by evaporation. After that mercury was pre-concentrated and purified from the matrix elements by eluting through another mini-size anion-exchange column. The matrix elements of concern included Co and Sn, as components of the methyl donors, Fe, as a component of the Fenton type reaction, and K, which arises from addition of elevated concentration of BrCl solution. The principle of Hg separation from matrix elements and preconcentration was similar to that used in previous approaches [12,32]. The anion-exchange resin AG-MP-1 M (Bio-Rad) was chosen as a cost-effective alternative to Chelex®-100 resin. The chromatographic columns were constructed from glass Pasteur pipettes fitted with plugs of cotton wool at their outlets and filled with ~0.2 ml of the 100–200 mesh size AG-MP-1 M anion-exchange resin. The columns were cleaned with 2 ml of 2 M HNO_3, rinsed with MQ-water and regenerated to the chloride forms with 3 ml of 1.5 M HCl. The solution of inorganic mercury was loaded onto the pre-conditioned column in 1.5 M HCl, further 1 ml of 1.5 M HCl were used to elute matrix elements followed by the elution of mercury by 2 ml of 0.1 M HNO_3 solution containing 0.15% L-cysteine and 0.001 M BrCl. All sample manipulations described above were performed in ultra-clean lab (Class-10). Total procedural blank of mercury (<0.1 ng) was found to be negligible relative to the amounts of mercury used in the experiments.

3. Results and discussion

3.1. Evaluation of performance of sample preparation procedures

Performance of chromatographic separation of methylmercury from inorganic mercury by using Chelex® 100 ion-exchange resin was described in detail in our previous study and need not be repeated here [12]. However, in the present study we introduced additional procedure including purification and preconcentration of the separated methylmercury from matrix elements by ion-exchange chromatography using AG-MP-1 M anion-exchange resin. The chromatographic separation of Hg can introduce bias in Hg isotope ratios due to incomplete recovery and co-elution of matrix components from the ion-exchange resin.

In order to make sure that none of the aforementioned processes introduces artificial Hg isotope fractionation, Hg isotope standard was repeatedly eluted through the chromatographic column, followed by Hg isotope ratio measurements by MC-ICPMS relative to the stock solution. The amount of Hg loaded onto the columns was 1.5 μg. Its quantitative recovery was ensured using aliquots of solutions taken before and after the anion-exchange separation. The recovery ranges from 96% to 102% ($n = 15$). Fig. 1 shows $\delta^{202/198}$Hg values of Hg isotope standard obtained after replicated elution. It can be seen from these data that $\delta^{202/198}$Hg values of Hg processed through the anion-exchange procedure are statistically indistinguishable from the long-term reproducibility of $\delta^{202/198}$Hg values for the stock solution of NIST-3133 isotope standard, the latter was assessed as 0.16‰ for $^{202/198}$Hg isotope ratio at two standard deviations level ($n = 25$).

3.2. Hg isotope ratio measurements in the methylation experiments

3.2.1. Reactions between inorganic Hg(II) and methylcobalamin in the dark

Methylcobalamin can be present in natural waters as a result of microbiological activity. The biological function of methylcobalamin is to act as an organometallic cofactor to facilitate enzymatic methyl transfer reactions. Methylcobalamin was also used previously as the methylating agent to quantitatively convert inorganic mercury into methylmercury in the laboratory experiments [33]. Detailed concentration and isotope data of mercury obtained in our experiments are given in Table 1.

Table 1
Concentration and isotope data obtained in the experiments. Hg isotope data are shown relative to the initial isotope composition of inorganic Hg. Uncertainty bars in isotope ratio data represent standard deviation of the mean between two replicate measurements at 95% confidence (2σ) level.

Measured fraction of MeHg	Hg isotope data of methylmercury, (‰) ± 2STD						Measured fraction of inorganic Hg	Hg isotope data of the remaining inorganic Hg, (‰) ± 2STD			
	$\delta^{199/198}$Hg	$\delta^{200/198}$Hg	$\delta^{201/198}$Hg	$\delta^{202/198}$Hg	Δ^{199}Hg	Δ^{201}Hg		$\delta^{199/198}$Hg	$\delta^{200/198}$Hg	$\delta^{201/198}$Hg	$\delta^{202/198}$Hg
Methylcobalamin as the methyl donor compound in the dark, pH = 5.0 ± 0.2											
0.05	−0.17 ± 0.04	−0.33 ± 0.06	−0.52 ± 0.08	−0.73 ± 0.09	0.01	0.03	0.95	0.02 ± 0.03	0.02 ± 0.04	0.05 ± 0.06	0.05 ± 0.08
0.10	−0.13 ± 0.06	−0.32 ± 0.07	−0.49 ± 0.09	−0.64 ± 0.10	0.03	−0.01	0.90	0.02 ± 0.05	0.05 ± 0.04	0.07 ± 0.08	0.09 ± 0.09
0.23	−0.16 ± 0.03	−0.30 ± 0.06	−0.46 ± 0.07	−0.67 ± 0.11	0.01	0.04	0.77	0.04 ± 0.04	0.10 ± 0.06	0.12 ± 0.07	0.20 ± 0.10
0.38	−0.12 ± 0.04	−0.26 ± 0.06	−0.41 ± 0.08	−0.51 ± 0.09	0.01	−0.03	0.62	0.06 ± 0.04	0.12 ± 0.07	0.15 ± 0.09	0.23 ± 0.10
0.53	−0.09 ± 0.04	−0.23 ± 0.07	−0.32 ± 0.09	−0.43 ± 0.12	0.02	0.01	0.47	0.12 ± 0.05	0.29 ± 0.06	0.43 ± 0.08	0.56 ± 0.09
0.67	−0.10 ± 0.05	−0.18 ± 0.07	−0.32 ± 0.08	−0.42 ± 0.10	0.01	−0.01	0.33	0.24 ± 0.03	0.42 ± 0.06	0.63 ± 0.07	0.88 ± 0.08
0.77	−0.09 ± 0.05	−0.14 ± 0.04	−0.23 ± 0.06	−0.29 ± 0.08	−0.02	−0.02	0.23	0.25 ± 0.03	0.47 ± 0.05	0.71 ± 0.07	0.98 ± 0.09
Methylcobalamin as the methyl donor compound in the presence of hydroxyl radicals in the dark, pH = 4.9 ± 0.3											
0.05	−0.30 ± 0.04	−0.55 ± 0.07	−0.83 ± 0.08	−1.13 ± 0.08	−0.01	0.03	0.95	0.03 ± 0.05	0.04 ± 0.07	0.03 ± 0.09	0.05 ± 0.10
0.11	−0.27 ± 0.03	−0.50 ± 0.05	−0.75 ± 0.10	−0.99 ± 0.12	−0.02	−0.01	0.89	0.02 ± 0.04	0.04 ± 0.04	0.05 ± 0.07	0.09 ± 0.09
0.13	−0.23 ± 0.05	−0.52 ± 0.06	−0.81 ± 0.09	−1.06 ± 0.14	0.03	−0.02	0.87	0.04 ± 0.04	0.04 ± 0.06	0.08 ± 0.08	0.13 ± 0.08
0.17	−0.22 ± 0.06	−0.46 ± 0.05	−0.68 ± 0.09	−0.94 ± 0.10	0.01	0.02	0.83	0.02 ± 0.03	0.12 ± 0.07	0.20 ± 0.09	0.24 ± 0.10
0.22	−0.24 ± 0.07	−0.46 ± 0.07	−0.67 ± 0.08	−0.90 ± 0.11	−0.02	0.01	0.78	0.08 ± 0.04	0.16 ± 0.05	0.24 ± 0.07	0.29 ± 0.08
0.19	−0.25 ± 0.03	−0.51 ± 0.06	−0.79 ± 0.11	−1.03 ± 0.13	0.01	−0.01	0.81	0.07 ± 0.05	0.11 ± 0.07	0.21 ± 0.08	0.24 ± 0.10
0.17	−0.25 ± 0.04	−0.49 ± 0.05	−0.78 ± 0.07	−1.08 ± 0.08	0.02	0.03	0.83	0.08 ± 0.04	0.13 ± 0.04	0.16 ± 0.08	0.22 ± 0.09
0.29	−0.20 ± 0.05	−0.34 ± 0.06	−0.52 ± 0.08	−0.75 ± 0.09	−0.01	0.04	0.71	0.09 ± 0.06	0.18 ± 0.05	0.26 ± 0.07	0.31 ± 0.08
0.48	−0.14 ± 0.06	−0.28 ± 0.06	−0.41 ± 0.07	−0.58 ± 0.06	0.01	0.03	0.52	0.12 ± 0.05	0.28 ± 0.07	0.37 ± 0.04	0.53 ± 0.06
0.58	−0.10 ± 0.04	−0.18 ± 0.07	−0.23 ± 0.09	−0.33 ± 0.10	−0.02	0.02	0.42	0.14 ± 0.04	0.27 ± 0.03	0.36 ± 0.05	0.46 ± 0.09
0.75	−0.08 ± 0.05	−0.15 ± 0.06	−0.18 ± 0.08	−0.25 ± 0.12	−0.02	0.01	0.25	0.18 ± 0.05	0.37 ± 0.04	0.51 ± 0.07	0.69 ± 0.08
Monomethyltin as the methyl donor compound in the dark, pH = 9.2 ± 0.4											
0.02	−0.26 ± 0.07	−0.45 ± 0.04	−0.68 ± 0.05	−0.90 ± 0.09	−0.03	−0.01	0.98	0.02 ± 0.03	0.03 ± 0.04	0.02 ± 0.04	0.05 ± 0.06
0.03	−0.20 ± 0.06	−0.35 ± 0.06	−0.53 ± 0.08	−0.74 ± 0.10	−0.01	0.02	0.97	0.01 ± 0.04	0.01 ± 0.06	−0.01 ± 0.07	0.01 ± 0.09
0.04	−0.23 ± 0.02	−0.41 ± 0.04	−0.61 ± 0.07	−0.84 ± 0.08	−0.02	0.02	0.96	0.02 ± 0.06	−0.01 ± 0.05	0.01 ± 0.06	0.07 ± 0.08
0.05	−0.19 ± 0.04	−0.35 ± 0.05	−0.52 ± 0.06	−0.73 ± 0.08	−0.01	0.02	0.95	0.01 ± 0.07	0.00 ± 0.06	0.01 ± 0.08	0.01 ± 0.09
0.06	−0.17 ± 0.04	−0.40 ± 0.07	−0.60 ± 0.08	−0.82 ± 0.09	0.03	0.02	0.94	0.01 ± 0.06	0.03 ± 0.07	0.07 ± 0.08	0.08 ± 0.10
0.08	−0.17 ± 0.05	−0.38 ± 0.05	−0.51 ± 0.07	−0.72 ± 0.09	0.01	0.03	0.92	0.01 ± 0.03	0.00 ± 0.06	0.02 ± 0.07	0.05 ± 0.09
0.07	−0.15 ± 0.06	−0.29 ± 0.04	−0.49 ± 0.06	−0.60 ± 0.08	0.0	−0.04	0.93	0.03 ± 0.06	0.01 ± 0.08	0.03 ± 0.07	0.05 ± 0.10
0.09	−0.20 ± 0.04	−0.35 ± 0.07	−0.52 ± 0.08	−0.72 ± 0.10	−0.02	0.02	0.91	−0.02 ± 0.04	0.03 ± 0.07	0.02 ± 0.06	0.06 ± 0.08
0.06	−0.19 ± 0.05	−0.31 ± 0.06	−0.46 ± 0.08	−0.60 ± 0.09	−0.01	−0.01	0.94	−0.02 ± 0.05	0.04 ± 0.06	0.04 ± 0.08	0.07 ± 0.09
0.07	−0.18 ± 0.06	−0.34 ± 0.08	−0.50 ± 0.08	−0.74 ± 0.07	0.01	0.05	0.93	0.02 ± 0.03	0.03 ± 0.04	0.03 ± 0.04	0.05 ± 0.07
0.06	−0.16 ± 0.03	−0.26 ± 0.05	−0.38 ± 0.07	−0.53 ± 0.08	−0.03	0.02	0.94	0.04 ± 0.06	−0.02 ± 0.06	0.04 ± 0.08	0.07 ± 0.04
Acetic acid as the methyl donor compound in the presence of hydroxyl radicals in the dark, pH = 5.1 ± 0.2											
0.01	−0.32 ± 0.04	−0.66 ± 0.06	−0.98 ± 0.06	−1.33 ± 0.08	0.02	0.02	0.99	0.00 ± 0.04	0.01 ± 0.05	0.02 ± 0.03	0.02 ± 0.06
0.01	−0.32 ± 0.06	−0.64 ± 0.07	−0.93 ± 0.08	−1.27 ± 0.10	−0.01	0.02	0.99	0.01 ± 0.06	−0.01 ± 0.05	−0.01 ± 0.07	0.00 ± 0.08
0.02	−0.34 ± 0.03	−0.60 ± 0.05	−0.94 ± 0.07	−1.22 ± 0.09	−0.03	−0.02	0.98	−0.02 ± 0.03	0.00 ± 0.07	0.00 ± 0.06	0.01 ± 0.08
0.02	−0.33 ± 0.04	−0.68 ± 0.04	−1.07 ± 0.06	−1.39 ± 0.08	0.02	−0.02	0.98	0.01 ± 0.04	0.04 ± 0.06	0.02 ± 0.08	0.04 ± 0.07
0.03	−0.35 ± 0.06	−0.67 ± 0.06	−0.96 ± 0.08	−1.27 ± 0.09	−0.03	−0.01	0.97	0.01 ± 0.02	0.00 ± 0.05	−0.02 ± 0.07	0.00 ± 0.06
0.04	−0.31 ± 0.05	−0.62 ± 0.06	−0.98 ± 0.08	−1.25 ± 0.07	0.00	−0.03	0.96	0.02 ± 0.04	0.04 ± 0.06	0.04 ± 0.08	0.07 ± 0.09
0.05	−0.38 ± 0.07	−0.66 ± 0.06	−1.07 ± 0.09	−1.40 ± 0.11	−0.03	−0.02	0.95	−0.01 ± 0.06	0.03 ± 0.07	0.02 ± 0.06	0.05 ± 0.10
0.04	−0.33 ± 0.06	−0.59 ± 0.08	−0.86 ± 0.07	−1.20 ± 0.10	−0.03	0.04	0.96	0.02 ± 0.04	0.03 ± 0.05	0.04 ± 0.06	0.05 ± 0.08
0.05	−0.28 ± 0.05	−0.51 ± 0.06	−0.80 ± 0.08	−1.09 ± 0.09	−0.01	0.02	0.95	0.03 ± 0.03	−0.02 ± 0.06	0.02 ± 0.08	−0.03 ± 0.08
0.04	−0.30 ± 0.08	−0.56 ± 0.07	−0.81 ± 0.09	−1.07 ± 0.12	−0.03	−0.01	0.96	−0.02 ± 0.05	−0.03 ± 0.04	−0.03 ± 0.06	−0.04 ± 0.07
0.04	−0.27 ± 0.06	−0.52 ± 0.08	−0.77 ± 0.10	−0.95 ± 0.13	−0.03	−0.06	0.96	−0.02 ± 0.04	0.03 ± 0.06	0.07 ± 0.07	0.08 ± 0.09

Table 1 (*Continued*)

Measured fraction of MeHg	Hg isotope data of methylmercury, (‰) ± 2STD						Measured fraction of inorganic Hg	Hg isotope data of the remaining inorganic Hg, (‰) ± 2STD			
	$\delta^{199/198}$Hg	$\delta^{200/198}$Hg	$\delta^{201/198}$Hg	$\delta^{202/198}$Hg	Δ^{199}Hg	Δ^{201}Hg		$\delta^{199/198}$Hg	$\delta^{200/198}$Hg	$\delta^{201/198}$Hg	$\delta^{202/198}$Hg
Dimethylsulfoxide as the methyl donor compound in the presence of hydroxyl radicals in the dark, pH = 4.8 ± 0.4											
0.010	−0.27 ± 0.04	−0.52 ± 0.04	−0.78 ± 0.07	−1.02 ± 0.08	−0.01	−0.01	0.99	0.01 ± 0.03	0.03 ± 0.04	0.03 ± 0.04	0.06 ± 0.07
0.022	−0.21 ± 0.05	−0.44 ± 0.06	−0.68 ± 0.07	−0.89 ± 0.09	0.01	−0.01	0.97	0.03 ± 0.06	0.04 ± 0.05	0.06 ± 0.04	0.09 ± 0.08
0.024	−0.27 ± 0.06	−0.53 ± 0.04	−0.73 ± 0.05	−1.01 ± 0.07	−0.01	0.03	0.95	0.01 ± 0.04	0.03 ± 0.07	0.02 ± 0.06	0.02 ± 0.08
0.031	−0.25 ± 0.06	−0.40 ± 0.06	−0.62 ± 0.07	−0.80 ± 0.12	−0.05	−0.02	0.94	0.03 ± 0.05	0.04 ± 0.06	0.04 ± 0.06	0.06 ± 0.09
0.033	−0.24 ± 0.07	−0.52 ± 0.08	−0.82 ± 0.09	−1.07 ± 0.14	0.03	−0.01	0.96	0.00 ± 0.04	0.02 ± 0.06	0.02 ± 0.07	0.02 ± 0.08
0.032	−0.26 ± 0.06	−0.47 ± 0.09	−0.74 ± 0.07	−0.99 ± 0.10	−0.02	0.00	0.95	0.01 ± 0.06	0.03 ± 0.04	0.01 ± 0.07	0.03 ± 0.10
0.040	−0.25 ± 0.05	−0.47 ± 0.06	−0.60 ± 0.08	−0.83 ± 0.09	−0.04	0.02	0.93	−0.02 ± 0.04	−0.01 ± 0.04	0.02 ± 0.05	0.03 ± 0.08
0.032	−0.16 ± 0.06	−0.35 ± 0.04	−0.52 ± 0.08	−0.74 ± 0.08	0.03	0.04	0.98	0.02 ± 0.06	0.03 ± 0.07	0.05 ± 0.08	0.08 ± 0.10
0.035	−0.26 ± 0.04	−0.49 ± 0.05	−0.74 ± 0.06	−0.99 ± 0.07	−0.01	0.01	0.95	0.00 ± 0.06	0.02 ± 0.04	0.06 ± 0.06	0.08 ± 0.09
0.022	−0.16 ± 0.07	−0.37 ± 0.08	−0.59 ± 0.06	−0.84 ± 0.10	0.05	0.04	0.94	0.03 ± 0.05	0.05 ± 0.06	0.08 ± 0.08	0.11 ± 0.10
0.030	−0.18 ± 0.04	−0.34 ± 0.06	−0.67 ± 0.08	−0.80 ± 0.11	0.02	−0.07	0.96	−0.02 ± 0.04	0.01 ± 0.06	−0.03 ± 0.07	−0.05 ± 0.09
Photochemical methylation using methylcobalamin as the methyl donor compound, pH = 5											
0.0015	0.17 ± 0.03	−0.26 ± 0.04	−0.16 ± 0.05	−0.52 ± 0.05	0.30	0.24	0.991	−0.01 ± 0.07	0.01 ± 0.04	−0.02 ± 0.08	0.02 ± 0.10
0.0022	0.24 ± 0.04	−0.19 ± 0.04	0.02 ± 0.07	−0.35 ± 0.06	0.33	0.28	0.995	−0.01 ± 0.06	0.02 ± 0.07	0.01 ± 0.09	0.01 ± 0.11
0.0025	0.36 ± 0.04	−0.24 ± 0.06	0.02 ± 0.08	−0.48 ± 0.07	0.48	0.38	0.986	−0.02 ± 0.05	0.02 ± 0.06	−0.01 ± 0.07	0.02 ± 0.10
0.0036	0.39 ± 0.05	−0.26 ± 0.04	0.03 ± 0.07	−0.50 ± 0.05	0.52	0.41	n.d.	n.d.	n.d.	n.d.	n.d.
0.0047	0.37 ± 0.06	−0.24 ± 0.04	0.06 ± 0.06	−0.46 ± 0.07	0.48	0.41	n.d.	n.d.	n.d.	n.d.	n.d.
0.0051	0.45 ± 0.04	−0.28 ± 0.06	0.06 ± 0.05	−0.58 ± 0.08	0.60	0.50	n.d.	n.d.	n.d.	n.d.	n.d.
Photochemical methylation using acetic acid as the methyl donor compound, pH = 5											
0.0010	0.20 ± 0.06	−0.23 ± 0.07	−0.06 ± 0.06	−0.41 ± 0.08	0.30	0.25	0.994	0.00 ± 0.03	0.02 ± 0.04	0.01 ± 0.04	0.01 ± 0.07
0.0032	0.31 ± 0.05	−0.21 ± 0.04	−0.01 ± 0.08	−0.45 ± 0.06	0.42	0.33	0.987	−0.01 ± 0.04	0.01 ± 0.05	−0.03 ± 0.04	0.02 ± 0.08
0.0040	0.39 ± 0.04	−0.19 ± 0.06	0.16 ± 0.08	−0.35 ± 0.09	0.48	0.42	0.989	−0.02 ± 0.05	−0.01 ± 0.04	−0.02 ± 0.07	0.02 ± 0.08
0.0038	0.41 ± 0.04	−0.28 ± 0.05	0.05 ± 0.06	−0.55 ± 0.09	0.55	0.46	n.d.	n.d.	n.d.	n.d.	n.d.
0.0045	0.52 ± 0.06	−0.27 ± 0.03	0.12 ± 0.07	−0.50 ± 0.08	0.65	0.50	n.d.	n.d.	n.d.	n.d.	n.d.
0.0049	0.52 ± 0.05	−0.20 ± 0.06	0.24 ± 0.06	−0.38 ± 0.10	0.62	0.53	n.d.	n.d.	n.d.	n.d.	n.d.

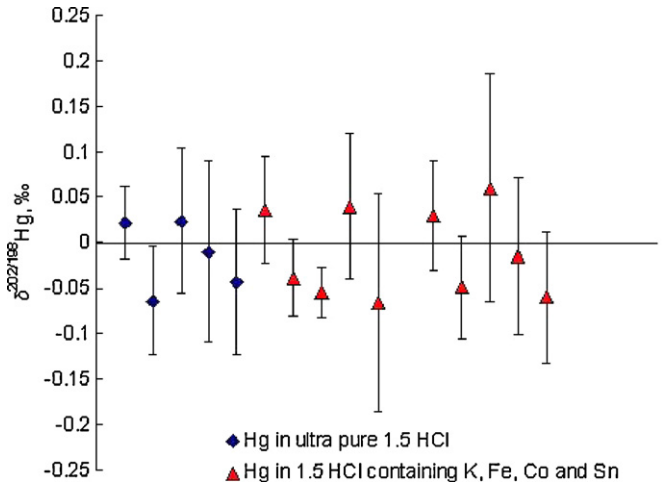

Fig. 1. Reproducibility of $\delta^{202/198}$Hg values after replicated elution of the Hg isotope standard through chromatographic columns prepared from AG-MP-1 M anion-exchange resin in solution of ultrapure 1.5 M HCl (diamonds) and in solution of 1.5 M HCl containing K, Fe, Co and Sn each at concentration of ~20 μg/ml (triangles). Uncertainty bars are standard deviations of the measurements at 95% confidence (2σ) level.

Yield of methylmercury plotted as a function of time is shown in Fig. 2a. An efficient conversion of inorganic Hg(II) into methylmercury was observed in the experiments both with and without hydroxyl radicals in solution. As seen from Fig. 2b, the lighter Hg isotopes preferentially partition into methylmercury during methylation. This fractionation was found to be mass-dependent with the Δ^{199}Hg and Δ^{201}Hg values are within the limits of instrumental uncertainty (Table 1). It is worth noting that the measured concentrations and isotope ratios of both methylmercury and parent inorganic mercury agree very well with mass balance calculations.

An interesting observation is that both rate of methylmercury formation and magnitude of Hg isotope fractionation in the beginning of the experiments are higher in the presence of the hydroxyl radicals than without them. A trivial explanation of this observation is that different mechanisms of a methyl group transfer occur in these experiments. There is sufficient evidence published to suggest that in the absence of microorganisms the transfer of a methyl group to mercury as carbanion (CH_3^-) is the most plausible mechanism [34,35]. This can be described as follows [18]:

$$CH_3\text{–}Co(III) \rightarrow [CH_3^-] + Co(III) \quad (7)$$

On the other hand, a homolytic cleavage of CH_3–Co bond according to the reaction scheme (8) can occur in the presence of the hydroxyl radicals in solution, resulting in the release of a methyl radical ($CH_3^\bullet$) into solution [18]

$$CH_3\text{–}Co(III) \rightarrow [CH_3^\bullet] + Co(II) \quad (8)$$

Thus, it seems likely that in the presence of hydroxyl radicals in solution the pathways of the reaction change with the transfer of a CH_3 group to mercury as a methyl radical becoming more important one.

In the experiments without hydroxyl radicals, the $\delta^{202/198}$Hg values plotted against fraction of inorganic mercury are closely approximated by Rayleigh curves constructed by using Eq. (5) and kinetic isotope fractionation factor, α^K, of 0.9993 inferred from the experimental data of the experiments without radicals (Fig. 2c). It is worth noting that Eq. (5) can be written in the form of a linear equation in which the straight line passes through zero

$$y = bx \quad (9)$$

where $y = \ln((10^{-3}\delta_s + 1)/(10^{-3}\delta_{s,0} + 1))$, $x = \ln f$, and $b = (\alpha^K - 1)$.

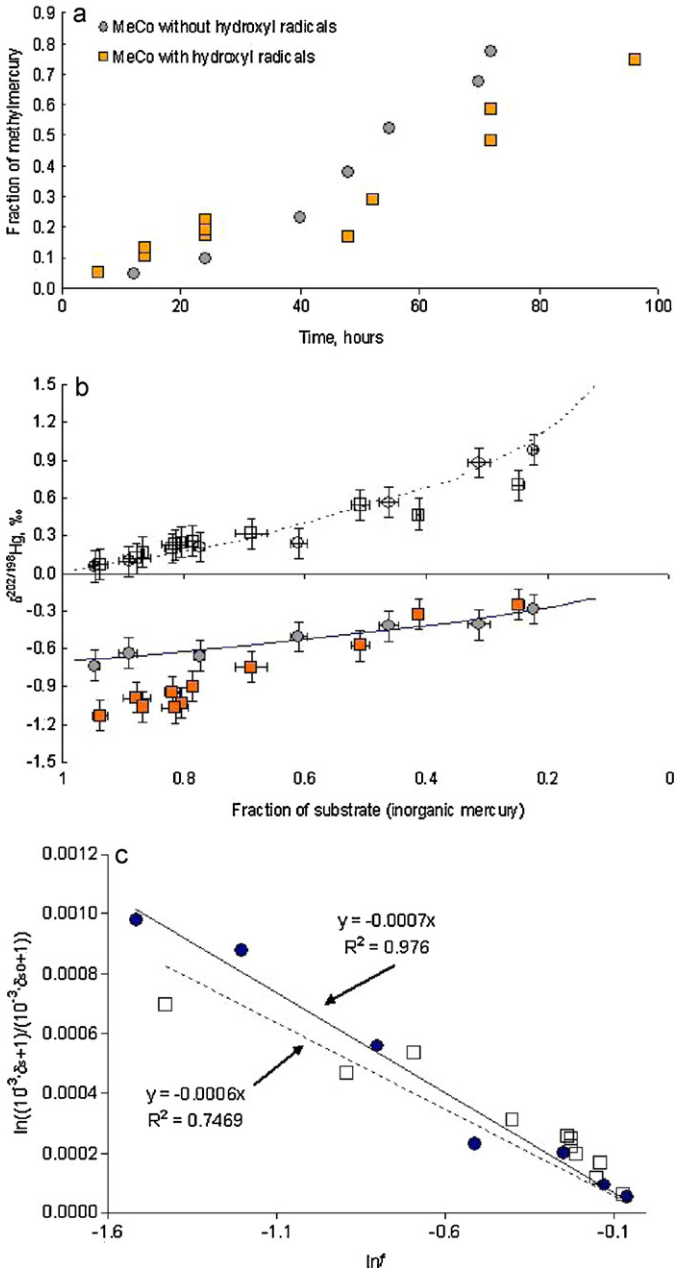

Fig. 2. Summary of Hg concentration and $\delta^{202/198}$Hg values in the experiments with methylcobalamin. Section (a) represents the yield of methylmercury plotted versus time of the experiments. Section (b) shows $\delta^{202/198}$Hg values of both methylmercury and inorganic mercury plotted versus fraction of inorganic mercury in the experiments without hydroxyl radicals (circles) and with hydroxyl radicals (squares). Open symbol represent the data for inorganic mercury. Filled symbols represent the data for methylmercury. Fraction of inorganic mercury plotted in the graphs has been calculated as the mean between measured values of remaining inorganic mercury and a value calculated from measured methylmercury. Uncertainty bars are standard deviations of the aforementioned mean at 70% confidence (1σ) level. Dashed and solid lines are Rayleigh curves for the substrate and the product, respectively, which were constructed by using Eq. (5) and the inferred kinetic isotope fractionation factor of 0.9993 (see below). Section (c) illustrates a plot of $\delta^{202/198}$Hg values versus fraction of inorganic mercury in the ln–ln space which was used to infer kinetic isotope fractionation factor in the experiments without hydroxyl radicals (circles) and in the presence of hydroxyl radicals (squares). Dashed and solid lines represent linear regression of data points in the experiments with and without radicals, respectively (see also text for details). Uncertainty bars for $\delta^{202/198}$Hg values are standard deviations of the measurements at 95% confidence (2σ) level.

The slope in Eq. (9) is also known as enrichment factor of the product relative to the substrate and denoted in per mil notation as $e = 1000(\alpha^K - 1)$ [24,25].

By using the experimental data and plotting $\ln((10^{-3}\delta_s + 1)/(10^{-3}\delta_{s,0} + 1))$ versus $\ln f$, it is possible to get an idea about significance of kinetic isotope fractionation in a single unidirectional reaction. Regression analysis shows that distribution of data points in the experiments without radicals in $\ln((10^{-3}\delta_s + 1)/(10^{-3}\delta_{s,0} + 1))$ versus $\ln f$ space is well described by a straight line forced through the origin, with the *R*-squared value of 0.976 (Fig. 2c). This indicates that kinetic isotope effect during a single stage of the process of methylation of mercury by methylcobalamin predominantly controls Hg isotope fractionation under the conditions employed in the experiments. Kinetic isotope fractionation factor $\alpha^K = 0.9993$ in this process can be easily calculated from Eq. (9).

In contrast, Hg isotope fractionation during methylation in the presence of hydroxyl radicals is poorer approximated by a linear regression through the data points in $\ln((10^{-3}\delta_s + 1)/(10^{-3}\delta_{s,0} + 1))$ versus $\ln f$ space with the *R*-squared value of 0.7469 (Fig. 2c). This suggests that several processes contribute to the observed Hg isotope fractionation. It is known that highly reactive hydroxyl radicals generated in the experimental solutions can attack the new-formed methylmercury, leading to its dissociation. Thus, methylmercury formed in the presence of hydroxyl radicals is the net result of simultaneously occurring methylation and demethylation processes. Among the processes contributing to the observed Hg isotope fractionation in the experiments with radicals can therefore be kinetic isotope effects operating during both methylation and demethylation of mercury. In addition, equilibrium isotope fractionation can also take place in these reactions.

It is known that methylmercury can react further with methylcobalamin to produce dimethylmercury, $(CH_3)_2Hg$, but the reaction rate of this reaction has been reported to be much slower than the reaction of inorganic Hg(II) with methylcobalamin [34].

3.2.2. Reactions between inorganic Hg(II) and monomethyltin in the dark

Transmethylation reaction between organometallic species containing alkyl groups and mercury are among the most important chemical pathways for abiotic methylation of mercury [1,36]. Methyltin and its higher alkylated species have received significant attention as methyl donors in transmethylation reactions because of the wide industrial use of organotin compounds including applications as antifouling paints, fungicides, plastic and timber stabilizers [37]. Apart from sources of anthropogenic pollution, monomethyltin is naturally produced [17,37]. Reported average concentration of monomethyltin is 0.63 ng/l in seawater and 2.0 ng/l in freshwater [17]. These concentrations are similar to those of dissolved mercury in natural waters with the average concentration of 0.5 ± 0.3 ng/l reported for North Atlantic Ocean [38] and the wide range of values from 0.37 ng/l to tens ng/l in fresh water [17].

In the simplest form, the transmethylation reaction between inorganic Hg and monomethyltin in the presence of chloride can be described as follows:

$$MeSnCl_3 + HgCl_2 \rightarrow MeHgCl + SnCl_4 \quad (10)$$

Previous studies demonstrated that the reaction rate depends strongly on pH and is the most efficient in alkaline medium, which was chosen in our experiments [36]. All data obtained in the experiments can be found in Table 1. Yield of methylmercury plotted against time and $\delta^{202/198}$Hg values plotted against fraction of inorganic mercury are shown in Fig. 3. As seen from Fig. 3a, methylation of mercury by monomethyltin was much less efficient in comparison with methylcobalamin. After converting of ~5 to 8% of inorganic Hg(II) into methylmercury during first 24 h the yield of

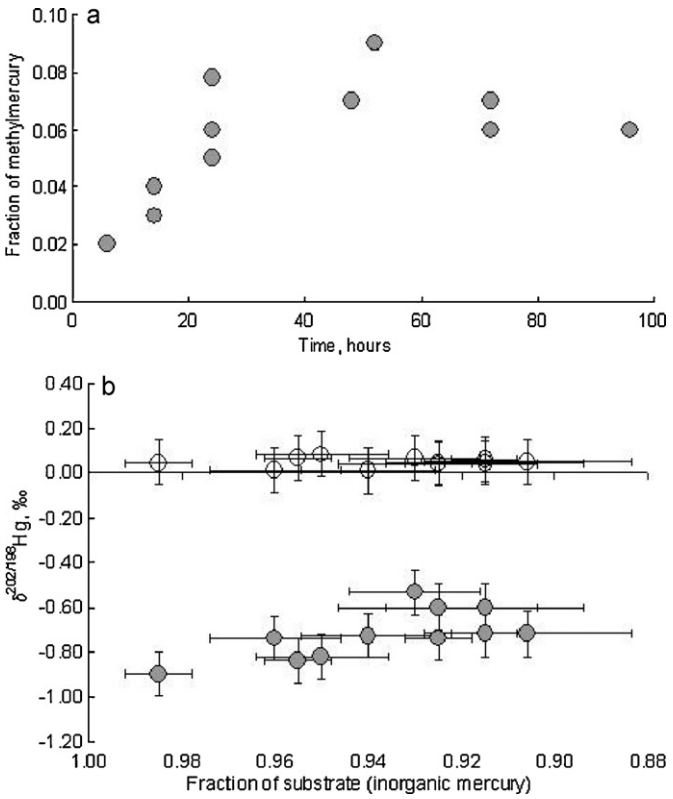

Fig. 3. Summary of Hg concentration and $\delta^{202/198}$Hg values in the experiments with monomethyltin without hydroxyl radicals. Section (a) shows the yield of methylmercury plotted versus time. Section (b) shows $\delta^{202/198}$Hg values of methylmercury (filled symbols) and inorganic mercury (open symbols) plotted versus fraction of inorganic mercury. The latter has been calculated as the mean between measured values of remaining inorganic mercury and a value calculated from measured methylmercury. Uncertainty bars for Hg concentration data are standard deviations of the aforementioned mean at 70% confidence (1σ) level. Uncertainty bars for $\delta^{202/198}$Hg values are standard deviations of the measurements at 95% confidence (2σ) level.

methylation did not change significantly further with time. This suggests that a sort of equilibrium was established in partitioning of methyl groups between mercury and tin. It is therefore impossible to determine a single kinetic isotope fractionation factor which could be a constant over the entire process of methylation.

Hg isotope composition of methylmercury formed is lighter than that of the inorganic source with instantaneous isotope fractionation factors, α^l, in terms of $^{202}Hg/^{198}Hg$ ratio ranging from 0.9991 to 0.9994. Both kinetic and equilibrium isotope effects can contribute to the observed Hg isotope fractionation. The isotope fractionation was found to be mass-dependent with the Δ^{199}Hg and Δ^{201}Hg values remaining within the limits of analytical uncertainty (Table 1).

The presence of hydroxyl radicals produced by the Fenton type reaction resulted in strong inhibition of methylmercury formation. In spite of the attempts to optimize the process by producing less amounts of hydroxyl radicals, the detected amounts of methylmercury were lower than 1 ng. These amounts of methylmercury were not sufficient for reliable Hg isotope analysis. The observed inhibition of methylmercury formation is presumably explained by that the coordination position on the mercury occupied by the methyl group is taken up by the highly reactive hydroxyl radical.

3.2.3. Reactions of inorganic Hg(II) with acetic acid in the dark

It has been documented previously that reaction between inorganic Hg(II) and small organic molecules, including acetic acid, results in methylation of mercury [39]. The experiments with excess acetic acid as methyl donor have been performed in this

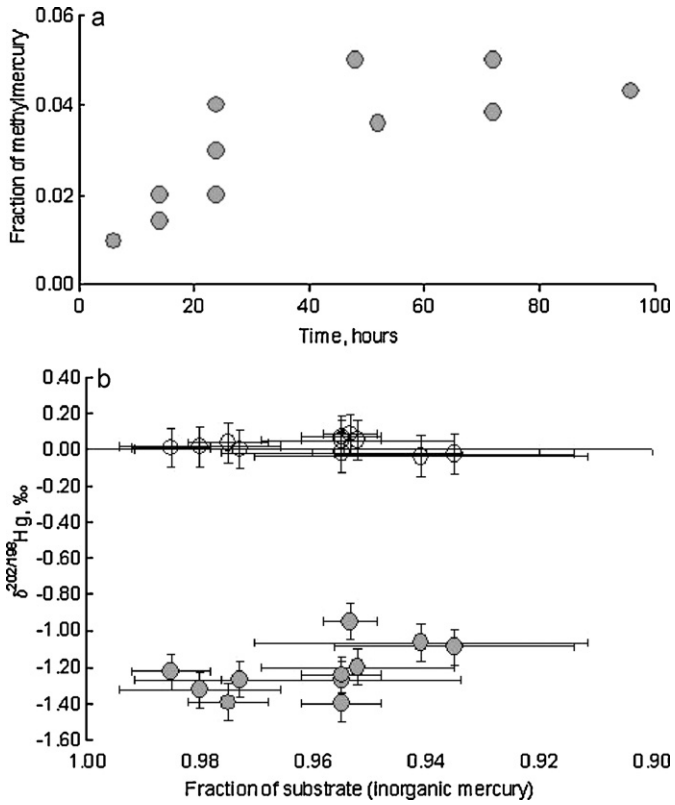

Fig. 4. Summary of Hg concentration and $\delta^{202/198}$Hg values in the experiments with acetic acid in the presence of hydroxyl radicals. Section (a) shows the yield of methylmercury plotted versus time. Section (b) shows $\delta^{202/198}$Hg values of methylmercury (filled symbols) and inorganic mercury (open symbols) plotted versus fraction of inorganic mercury. The latter has been calculated as the mean between measured values of remaining inorganic mercury and a value calculated from measured methylmercury. Uncertainty bars for Hg concentration data are standard deviations of the aforementioned mean at 70% confidence (1σ) level. Uncertainty bars for $\delta^{202/198}$Hg values are standard deviations of the measurements at 95% confidence (2σ) level.

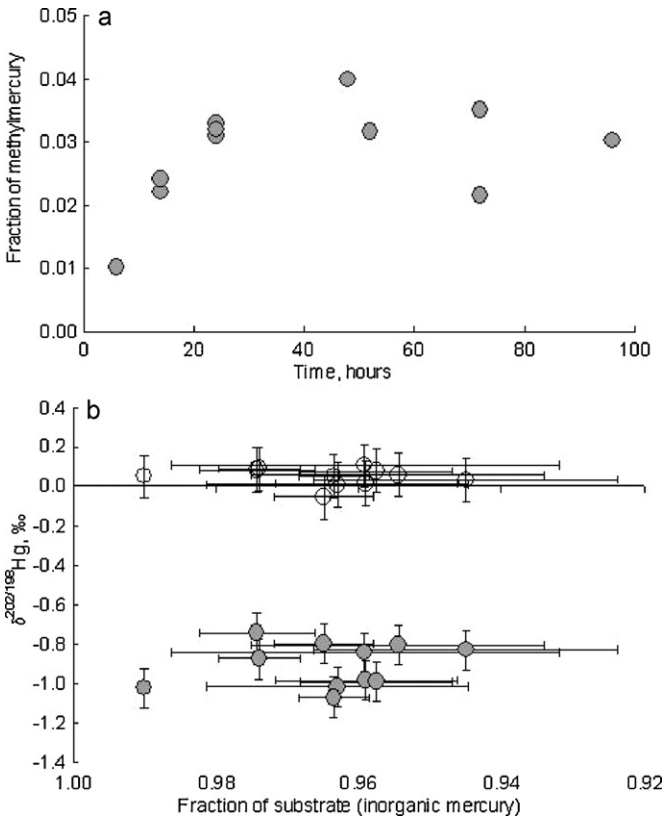

Fig. 5. Summary of Hg concentration and $\delta^{202/198}$Hg values in the experiments with dimethylsulfoxide in the presence of hydroxyl radicals. Section (a) shows the yield of methylmercury plotted versus time. Section (b) shows $\delta^{202/198}$Hg values of methylmercury (filled symbols) and inorganic mercury (open symbols) plotted versus fraction of inorganic mercury. The plotted fraction of inorganic mercury has been calculated as the mean between measured values of remaining inorganic mercury and a value calculated from measured methylmercury. Uncertainty bars for Hg concentration data are standard deviations of the aforementioned mean at 70% confidence (1σ) level. Uncertainty bars for $\delta^{202/198}$Hg values are standard deviations of the measurements at 95% confidence (2σ) level.

study at different pH values ranging from 5 to 9 in the dark. Trace amounts of methylmercury (less than 1 ng) relative to the source inorganic Hg have been produced in these experiments, being not sufficient for reliable Hg isotope ratio analysis. However, the methylation of mercury by acetic acid was found to be significantly more efficient in the presence of hydroxyl radicals in solution. This is presumably attributed to the fact that dissociation of acetic acid and mercuric acetate due to the radical attack yields a methyl radical according to the scheme [40]:

$$CH_3COOHgOCOCH_3 + [OH^\bullet] \rightarrow HOHgOCOCH_3 + [CH_3COO^\bullet] \quad (11)$$

$$[CH_3COO^\bullet] \rightarrow [CH_3^\bullet] + CO_2 \quad (12)$$

Fig. 4 provides a summary of the obtained concentration and isotope data. As seen from this figure, the plot of the yield of methylmercury versus time is similar to that from the experiments with methyltin in reaching a plateau after first 24 h. This shows that simultaneously occurring processes of methylation and demethylation equilibrated each other after approximately 5% of inorganic mercury was converted into methylmercury.

The isotopic composition of methylmercury is lighter than that of the inorganic source, with instantaneous isotope fractionation factors, α^I, in terms of $^{202}Hg/^{198}Hg$ ratio varying from 0.9985 to 0.9990. By analogy with the reaction with monomethyltin above, both kinetic and equilibrium isotope fractionation processes can contribute to the observed distribution of Hg isotopes. Hg isotope fractionation during the methylation by acetic acid shows the mass-dependent isotope pattern with undetectable MIF of Hg isotopes.

3.2.4. Reactions between inorganic Hg(II) and dimethylsulfoxide in the dark

Dimethylsulfoxide is produced in seawater by both photooxidation and bacterial transformation of dimethylsulfide [41]. We observed that reaction between inorganic mercury and dimethylsulfoxide without the presence of hydroxyl radicals yielded no detectable methylmercury. However, hydroxyl radicals are known to react with dimethylsulfoxide in the presence of oxygen to produce methyl and peroxomethyl radicals according to the following reactions [30]:

$$(CH_3)_2SO + OH^\bullet \rightarrow (CH_3)_2S^\bullet(O)OH \quad (13)$$

$$(CH_3)_2S^\bullet(O)OH \rightarrow CH_3S(O)OH + CH_3^\bullet \quad (14)$$

$$O_2 + CH_3^\bullet \rightarrow OOCH_3^\bullet \quad (15)$$

Fig. 5 shows a summary of the obtained concentration and isotope data in the experiments with the presence of radicals. Yield of methylmercury plotted against time resembles the pattern observed in the reactions with methyltin and acetic acid in reaching a plateau after converting a few percent of inorganic mercury into methylmercury. Instantaneous isotope fractionation factors, α^I, in terms of $^{202}Hg/^{198}Hg$ ratio vary from 0.9989 to 0.9993. Similar to that described above, different isotope fractionation pro-

cesses, including kinetic and equilibrium ones, can contribute to the observed variations in the isotope composition of mercury. Hg isotope fractionation during the reaction between inorganic mercury and DMSO was found to be mass-dependent with undetectable anomalies.

3.2.5. Photochemical methylation

Photodissociation of methyl group donor compounds results in releasing a methyl radical into solution. Using acetic acid as an example, the photodissociation reaction can be presented as follows [42,43]:

$$CH_3COOH + h\nu \rightarrow CH_3^{\bullet} + {}^{\bullet}COOH \quad (16)$$

A methyl radical can then reacts with inorganic Hg(II) to yield a molecule of methylmercury. An important aspect of the photochemical methylation is that it occurs simultaneously with photodegradation of methylmercury. Provided that there is sufficient concentration of a methyl donor compound in the solution, the efficiency of photoproduction versus photodegradation of methylmercury is dependent on kinetics of both processes.

An interesting observation is that only the reactions with methylcobalamin and acetic acid produced amounts of methylmercury, sufficient for reliable Hg isotope ratio determination. Traces of methylmercury have been measured in the experiments with methyltin and DMSO, but these quantities were less than 5 ng and not suitable for precise Hg isotope ratio analysis.

It is worth pointing out that both methylcobalamin and acetic acid can form stronger complexes with inorganic Hg(II) than methyltin and DMSO. Thus, the difference in methylation rate between the donor compounds can be explained by the so-called solvent cage effect. The latter implies that products of photodissociation of a methyl donor compound coordinated with mercury, including, among others, a methyl radical and inorganic Hg species (Hg^{2+} or Hg^{+}), are surrounded by molecules of solvent (H_2O). This cage greatly decreases the time needed for $CH_3^{\bullet}$ and Hg(II) to meet each other and increase the probability of that a chemical bond is established between them in the case of photo-assisted reactions with methylcobalamin and acetic acid. In contrast, in the case of a methyl donor compound not coordinated with mercury such as methyltin and DMSO, $CH_3^{\bullet}$ and Hg(II) need to travel longer distances in the bulk solution prior to their encounter to occur. This leads to that the predominant fraction of methyl radicals reacts with a third chemical species in solution, significantly decreasing the yield of the photochemical methylation.

Another interesting observation is that the photochemical methylation is accompanied by both the classical mass fractionation and mass-independent fractionation of Hg isotopes. Fig. 6 gives a summary of the obtained data in terms of $\delta^{202/198}$Hg values, Δ^{199}Hg values and Δ^{199}Hg/Δ^{201}Hg ratios. In contrast to previous figures, Hg isotope data in Fig. 6a and b have been plotted against fraction of methylmercury. This is because little amounts of methylmercury (less than 0.6%) were produced during photochemical methylation and the fraction of inorganic mercury Hg remained essentially constant at a level of the precision of Hg concentration measurements. The even Hg isotopes follow mass-dependent isotope fractionation with instantaneous isotope fractionation factors, α^{I}, ranging from 0.9994 to 0.9996 for the reactions with both methylcobalamin and acetic acid.

Mass-independent fractionation of Hg isotopes is displayed by pronounced enrichment of ^{199}Hg and ^{201}Hg isotopes relative to the even isotopes in methylmercury. It has been shown previously that photodissociation of dissolved methylmercury was accompanied by mass-independent fractionation of Hg isotopes due to the magnetic isotope effect [12]. The direction and magnitude of mass-independent fractionation of ^{199}Hg and ^{201}Hg isotopes observed in this study also suggest that the magnetic isotope effect is the plausible cause of the mass-independence of Hg isotope fractionation during photochemical methylation. As described in detail elsewhere [12,44], photodissociation of methylmercury via the radical pair mechanism involves the intersystem crossing from chemically inert triplet electronic state to chemically reactive singlet electronic state and leads to that the regeneration of methylmercury molecule is much more efficient in the radical pairs containing ^{199}Hg and ^{201}Hg isotopes. In the simultaneously occurring processes of photoproduction of methylmercury and its photodissociation, ^{199}Hg and ^{201}Hg isotopes are therefore continuously enriched in the fraction of methylmercury relative to the even isotopes. The slope obtained for the plot of Δ^{201}Hg versus Δ^{199}Hg is 1.247 ± 0.038 and consistent with a value suggested previously for the magnetic isotope effect [10].

Reactions involving radical intermediates are of primary importance during methylation/demethylation reactions in both

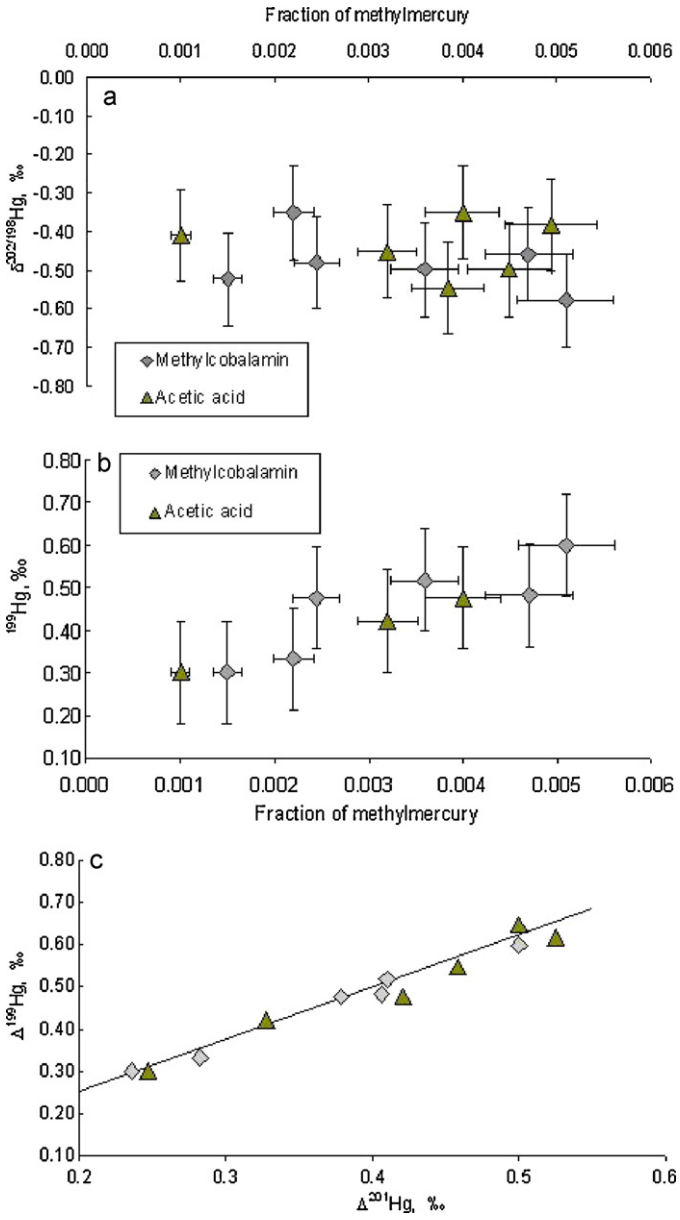

Fig. 6. $\delta^{202/198}$Hg and Δ^{199}Hg values plotted against fraction of methylmercury produced due to photochemical methylation of mercury in the presence of methylcobalamin and acetic acid (Sections (a) and (b), respectively). Section (c) shows a plot of Δ^{199}Hg versus Δ^{201}Hg values of methylmercury. Uncertainty bars are standard deviations of the measurements at 95% confidence (2σ) level.

photochemical experiments and the radical-assisted experiments in the dark. However, in contrast to the photochemical experiments, the methylation/demethylation reactions in the dark in the presence of hydroxyl radicals displayed only mass-dependent Hg isotope fractionation. We believe that the absence of Hg isotope anomalies during radical substitution reactions in the dark does not rule out formation of radical pairs during methylation/demethylation of mercury, but indicates that intensity of triplet–singlet intersystem crossing in radical pairs is not sufficient for measurable spin-selective Hg isotope effect to occur. In other words, a lack of energetic excitation is a plausible explanation for the absence of mass-independent Hg isotope fractionation during the radical-assisted methylation/demethylation reactions in the dark.

4. Conclusions

Data obtained in this study indicate that pure chemical, abiotic methylation of mercury is accompanied by fractionation of Hg isotopes. Methylation of mercury by various methyl group donors in the dark leads to mass-dependent Hg isotope fractionation with undetectable Hg isotope anomalies. In the light of the on-going discussion about the origin of MIF of Hg isotope an interesting observation was that the radical substitution reactions, producing methyl radical, could facilitate formation of methylmercury and increase the magnitude of the concomitant classical Hg isotope effect but were not capable of producing any measurable mass-independent Hg isotope fractionation.

In contrast to methylation in the dark, photochemical methylation of mercury was accompanied by both mass-dependent isotope fractionation and mass-independent fractionation of ^{199}Hg and ^{201}Hg isotopes. This mass-independence has been attributed to the magnetic isotope effect, operating during photodissociation of the produced methylmercury and resulting in the selective enrichment of methylmercury with ^{199}Hg and ^{201}Hg isotopes.

These findings have interesting implications in the field of biogeochemistry of mercury. They bring further evidence that it is the effect of irradiation by light that opens up additional reaction channels during transformations between different chemical forms of mercury and results in mass-independence of Hg isotope fractionation. Our data highlight the fact that apart from photochemical reduction, the light-assisted methylation/demethylation reactions can produce mass-independent isotope signature of Hg in the aquatic environments.

Acknowledgments

The staff of the Atomic & Mass Spectrometry Group, University of Ghent, is gratefully acknowledged for technical support. F.V. acknowledges the Flemish Research Foundation for financial support under the form of a research project. The authors are grateful to two anonymous referees for their constructive comments on the initial version of the manuscript.

References

[1] S.M. Ullrich, T.W. Tanton, S.A. Abdrashitova, Mercury in the aquatic environment: a review of factors affecting methylation, Crit. Rev. Environ. Sci. Technol. 31 (2001) 241–293.
[2] Global Mercury Assessment, Report by UNEP Chemicals, Geneva, 2002, http://www.chem.unep.ch/mercury/publications/default.htm.
[3] W.I. Ridley, S.J. Stetson, A review of isotopic composition as an indicator of the natural and anthropogenic behaviour of mercury, Appl. Geochem. 21 (2006) 1889–1899.
[4] T.A. Jackson, D.M. Whittle, M.S. Evans, C.G. Muir, Evidence for mass-independent and mass-dependent fractionation of the stable isotopes of mercury by natural processes in aquatic ecosystems, Appl. Geochem. 23 (2008) 547–571.
[5] B.A. Bergquist, J.D. Blum, The odds and evens of mercury isotopes: applications of mass-dependent and mass-independent isotope fractionation, Elements 5 (2009) 353–357.
[6] A. Biswas, J.D. Blum, B.A. Bergquist, G.J. Keeler, Z. Xie, Natural mercury isotope variation in coal deposits and organic soils, Environ. Sci. Technol. 42 (2008) 8303–8309.
[7] E.G. Gehrke, J.D. Blum, P. Meyers, The geochemical behaviour and isotopic composition of Hg in a mid-Pleistocene western Mediterranean sapropel, Geochim. Cosmochim. Acta 73 (2009) 1651–1665.
[8] B.A. Bergquist, J.D. Blum, Mass-dependent and -independent fractionation of Hg isotopes by photoreduction in aquatic systems, Science 318 (2007) 417–420.
[9] W. Zheng, H. Hintelmann, Nuclear field shift effect in isotope fractionation of mercury during abiotic reduction in the absence of light, J. Phys. Chem. A 114 (2010) 4238–4245.
[10] W. Zheng, H. Hintelmann, Isotope fractionation of mercury during its photochemical reduction by low-molecular-weight organic compounds, J. Phys. Chem. A 114 (2010) 4246–4253.
[11] N. Estrade, J. Carignan, J.E. Sonke, O.F.X. Donard, Mercury isotope fractionation during liquid–vapor evaporation experiments, Geochim. Cosmochim. Acta 73 (2009) 2693–2711.
[12] D. Malinovsky, K. Latruwe, L. Moens, F. Vanhaecke, Experimental study on mass-independence of Hg isotope fractionation during photodecomposition of dissolved methylmercury using MC-ICPMS, J. Anal. Atom. Spectrom. 25 (2010) 950–956.
[13] R. Das, V.J.M. Salters, A.L. Odom, A case for in vivo mass-independent fractionation of mercury isotopes in fish, Geochem. Geophys. Geosystem 10 (2009) Q11012.
[14] P. Rodriguez-Gonzalez, V.N. Epov, R. Bridou, E. Tessier, R. Guyoneaud, M. Monperrus, D. Amouroux, Species-specific stable isotope fractionation of mercury during Hg(II) methylation by an Anaerobic bacteria (Desulfobulbus propionicus) under dark conditions, Environ. Sci. Technol. 43 (2009) 9183–9188.
[15] K. Kritee, J.D. Blum, M.W. Johnson, B.A. Bergquist, T. Barkay, Mercury stable isotope fractionation during reduction of Hg(II) to Hg(0) by mercury resistant microorganisms, Environ. Sci. Technol. 41 (2007) 1889–1895.
[16] K. Kritee, T. Barkay, J.D. Blum, Mass dependent stable isotope fractionation of mercury during mer mediated microbial degradation of monomethylmercury, Geochim. Cosmochim. Acta 73 (2009) 1285–1296.
[17] T. Hamasaki, H. Nagase, Y. Yoshioka, T. Sato, Formation, distribution, and ecotoxicity of methylmetals of tin, mercury and arsenic in the environment, CRC Crit. Rev. Environ. Sci. Technol. 25 (1995) 45–91.
[18] B. Banerjee, S.W. Ragsdale, The many faces of vitamin B12: catalysis by cobalamin-dependent enzymes, Annu. Rev. Biochem. 72 (2003) 209–247.
[19] D. Malinovsky, R. Sturgeon, L. Yang, Anion-exchange chromatographic separation of Hg for isotope ratio measurements by multicollector ICPMS, Anal. Chem. 80 (2008) 2548–2555.
[20] D.C. Baxter, I. Rodushkin, E. Engstrom, D. Malinovsky, Revised exponential model for mass bias correction using an internal standard for isotope abundance ratio measurements by multi-collector ICP-MS, J. Anal. Atom. Spectrom. 21 (2006) 427–430.
[21] J.D. Blum, B.A. Bergquist, Reporting of variations in the natural isotopic composition of mercury, Anal. Bioanal. Chem. 388 (2007) 353–359.
[22] E.D. Young, A. Galy, H. Hagahara, Kinetic and equilibrium mass-dependent isotope fractionation laws in nature and their geochemical and cosmochemical significance, Geochim. Cosmochim. Acta 66 (2002) 1095–1104.
[23] J.L. Skulan, B.L. Beard, C.M. Johnson, Kinetic and equilibrium Fe isotope fractionation between aqueous Fe(III) and hematite, Geochim. Cosmochim. Acta 66 (2002) 2995–3015.
[24] A. Marriotti, J.C. Germon, P. Hubert, P. Kaiser, R. Letolle, A. Tardieux, P. Tardieux, Experimental determination of nitrogen kinetic isotope fractionation: some principles; illustration for the denitrification and nitrification process, Plant Soil 62 (1981) 413–430.
[25] M. Elsner, L. Zwank, D. Hunkeler, R.P. Schwarzenbach, A new concept linking observable stable isotope fractionation to transformation pathways of organic pollutants, Environ. Sci. Technol. 39 (2005) 6896–6916.
[26] R.J. Watts, M. Asce, A.L. Teel, Chemistry of modified Fenton's reagent (catalyzed H_2O_2 propagations –CHP) for in situ soil and groundwater remediation, J. Environ. Eng. 131 (2005) 612–622.
[27] G.V. Buxton, C.L. Greenstock, W.P. Helman, A.B. Ross, Critical review of rate constants for reactions of hydrated electrons, hydrogen atoms and hydroxyl radicals in aqueous solution, J. Phys. Chem. Ref. Data 17 (1988) 513–533.
[28] M.P. Jensen, J. Halpern, Dealkylation of coenzyme B12 and related organocobalamins: ligand structural effects on rates and mechanisms of hydrolysis, J. Am. Chem. Soc. 121 (1999) 2181–2192.
[29] F. De Smedt, X.V. Bui, T.L. Nguyen, J. Peeters, L. Vereecken, Theoretical and experimental study of the product branching in the reaction of acetic acid with OH radicals, J. Phys. Chem. A 109 (2005) 2401–2409.
[30] R. Herscu-Kluska, A. Masarwa, M. Saphier, H. Cohen, D. Meyerstein, Mechanism of the reaction of radicals with peroxides and dimethyl sulfoxide in aqueous solution, Chem. Eur. J. 14 (2008) 5880–5889.
[31] S.D. Siciliano, N.J. O'Driscoll, R. Tordon, J. Hill, S. Beauchamp, D.R.S. Lean, Abiotic production of methylmercury by solar radiation, Environ. Sci. Technol. 39 (2005) 1071–1077.
[32] J. Chen, H. Hintelmann, B. Dimock, Chromatographic pre-concentration of Hg from dilute aqueous solutions for isotopic measurement by MC-ICP-MS, J. Anal. Atom. Spectrom. 25 (2010) 1402–1409.

[33] R. Rodríguez Martín-Doimeadios, T. Stoichev, E. Krupp, D. Amouroux, M. Holeman, O.F.X. Donard, Micro-scale preparation and characterization of isotopically enriched monomethylmercury, Appl. Organomet. Chem. 16 (2002) 610–615.
[34] S.M. Chemaly, The link between vitamin B12 and methylmercury: a review, S. Afr. J. Sci. 98 (2002) 568–572.
[35] B.W. Chen, T. Wang, Y.G. Yin, B. He, G.B. Jiang, Methylation of inorganic mercury by methylcobalamin in aquatic systems, Appl. Organomet. Chem. 21 (2007) 462–467.
[36] V. Celo, D.R.S. Lean, S.L. Scott, Abiotic methylation of mercury in the aquatic environment, Sci. Tot. Environ. 368 (2006) 126–137.
[37] M. Hoch, Organotin compounds in the environment – an overview, Appl. Geochem. 16 (2001) 719–743.
[38] W.F. Fitzgerald, C.H. Lamborg, C.R. Hammerschmidt, Marine biogeochemical cycling of mercury, Chem. Rev. 107 (2007) 641–662.
[39] K. Gårdfeldt, J. Munthe, D. Strömberg, O. Lindqvist, A kinetic study on the abiotic methylation of divalent mercury in the aqueous phase, Sci. Tot. Environ. 304 (2003) 127–136.
[40] Y.A. Ol'dekop, N.A. Maier, Decarboxylation of mercury salts of organic acids under the action of peroxides and ultraviolet radiation, Russ. Chem. Bull. 15 (1966) 1127–1132.
[41] A.J. Hynes, P.H. Wine, The atmospheric chemistry of dimethylsulfoxide (DMSO) kinetics and mechanism of the OH + DMSO reaction, J. Atmos. Chem. 24 (1996) 23–37.
[42] H.T. Kwon, S.K. Shin, S.K. Kim, H.L. Kim, C.R. Park, Photodissociation dynamics of acetic acid and trifluoroacetic acid at 193 nm, J. Phys. Chem. A 105 (2001) 6775–6779.
[43] L.M. Yang, M.B. Ray, L.E. Yu, Photooxidation of dicarboxylic acids. Part II. Kinetics, intermediates and field observations, Atmos. Environ. 42 (2008) 868–880.
[44] A.L. Buchachenko, Magnetic isotope effect: nuclear spin control of chemical reactions, J. Phys. Chem. A 105 (2001) 9995–10011.